TECHNICAL REPORT

CT-ED conversion on a GE Lightspeed-RT scanner: influence of scanner settings*

M.A. Ebert [1,2], J. Lambert [3] and P.B. Greer [3,4]

[1]*Department of Radiation Oncology, Sir Charles Gairdner Hospital, Nedlands, Australia*
[2]*School of Physics, University of Western Australia, Nedlands, Australia*
[3]*School of Mathematical and Physical Sciences, University of Newcastle, Newcastle, Australia*
[4]*Department of Radiation Oncology, Calvary Mater Newcastle Hospital, Newcastle, Australia*

Abstract

The influence of tube voltage (kV) and current (mA) on the resulting relationship of computed tomography number to electron density (CT-ED) was investigated for a wide-bore GE scanner. The influence of kV and mA scan settings were examined in combination with a 16-bit image reconstruction algorithm made available via the scanner software and which allowed resolution of CT numbers for high density materials. By using titanium and stainless steel inserts in an electron density phantom, mA variation was found to have minimal impact on the CT-ED relationship, whereas variation in kV led to significant differences in CT number for the high density materials. The scanner is also equipped with automatic tube-current modulation capabilities. The influence of automatic tube-current modulation on CT number was investigated for a range of materials in a phantom geometry. It was found that tube current modulation has negligible effect on CT number, though the changing dimension of the phantom did influence CT number of an aluminium insert for scans undertaken with both fixed and modulated tube currents. In light of evidence from other studies examining the influence of CT number on dose calculation, it is recommended that scanner settings and specific CT-ED look-up tables be considered when calculations will be required with high-density materials present.

Key words electron density, mA, automatic tube current modulation, computed tomography, radiotherapy

Introduction

The relationship between material electron density (ED) and image pixel intensity in computed tomography (CT) is used extensively by contemporary radiotherapy dose calculation algorithms[1-3]. This relationship is usually determined experimentally for specific settings of the scanner's X-ray tube kilovoltage (kV), beam current (mA) and possibly field-of-view (FOV), and the reconstruction algorithm used to determine pixel intensities from X-ray transmission measurements. By imaging a phantom containing sample materials of known electron densities, with those densities representing typical anatomical compositions, a CT-ED curve relevant to patient anatomy is obtained. The resulting CT-ED curve is used in radiotherapy planning when a patient is scanned with those particular scanner settings. It is advantageous if the same CT-ED curve can be used regardless of the settings used on the CT scanner at imaging.

There are certain situations in which it is necessary to alter the scanning settings. One is when there are materials in the patient which would normally extend outside the range of materials used in measurement of the CT-ED curve. These include high atomic number (Z) or high ED materials, such as materials used in the construction of prostheses[4-6].

Another such situation is when scanning techniques are used to dynamically modify the X-ray tube mA with position along the patient. Such automatic tube current modulation ('auto-mA', 'Smart-mA' etc) techniques are aimed at reducing the X-ray exposure patients receive by selecting mA according to average transmission at each point along a patient. The average transmission can be obtained from lateral and anterior scan localization (scout) images taken prior to axial scanning. These methods have been shown to reduce patient doses by in excess of 50 % without appreciable loss of image quality[7-12].

This study was aimed at examining the variation in CT-ED relationship with scanner tube and reconstruction settings in the context of data collection relevant to radiotherapy treatment planning. In particular, the ability of an extended-range reconstruction algorithm to provide indication of relative electron density above the normal region of linearity was studied, together with the relationship between phantom size, material density and

*Presented at EPSM-ABEC 2007, Fremantle Australia, October 14-18, 2007
Corresponding author: Martin A. Ebert, Dept of Radiation Oncology, Sir Charles Gairdner Hospital, Hospital Ave, Nedlands WA 6009 Australia, Email: Martin.Ebert@health.wa.gov.au
Received: 31 October 2007; Accepted: 23 April 2008

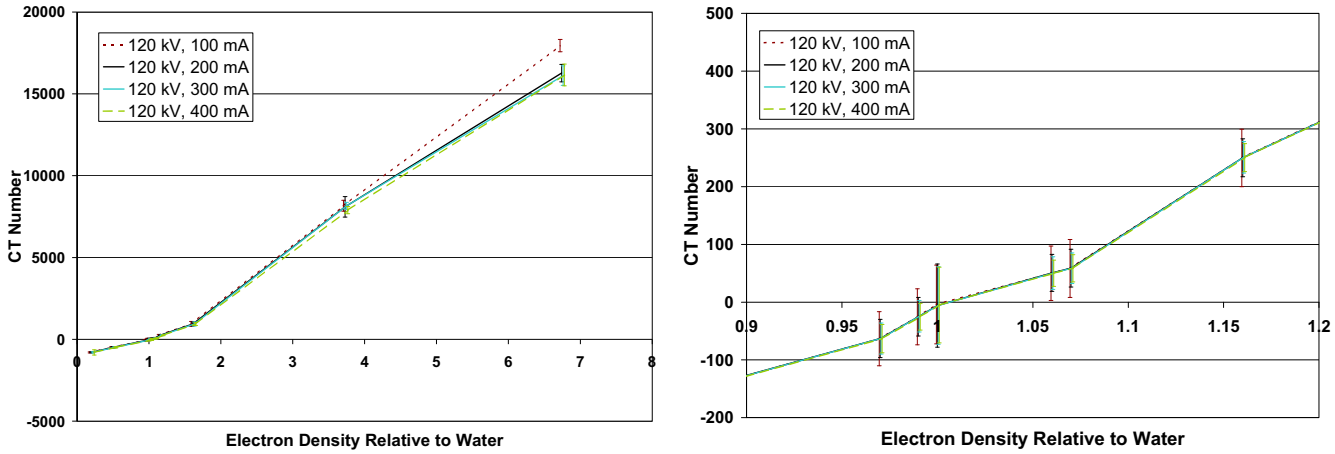

Figure 1. *CT-ED curves derived from images of the CIRS phantom with a variety of inserts for varying mA settings and a constant tube potential of 120 kV. a) Across the full range of relative electron densities considered. b) A magnification of the anatomically-relevant region of the curves (data points shifted slightly to make error bars distinguishable).*

resulting CT number when automatic tube-current modulation is employed.

Methods and results

Measurements were performed on a GE Lightspeed-RT scanner (GE Medical Systems, Milwaukee WI). The scanner has a large bore (80 cm) and performs 4-slice helical scanning. The scanner is used routinely for obtaining patient images for radiotherapy treatment planning at the Newcastle Mater Hospital (Newcastle, NSW)[†] and receives regular quality assurance (QA) for image quality and stability of the CT-ED relationship.

Images obtained on the scanner were exported to an eFilm (eFilm Digital Laboratories, Hollywood, CA) workstation where CT numbers and their standard deviation were obtained by examining the region of each image over the image slices through the centre of the phantom occupied by each material. Error bars represent the standard deviations for CT number in the region of interest for a single scan.

kV, mA and electron density

The scanner software includes an 'extended-range' reconstruction algorithm that involves reconstruction using 16-bit pixel intensities rather then the usual 12-bit, extending the representation of relative attenuation from (-1024 to +3071) to (-1024 to +64511)[‡]. This theoretically permits an extension of the linear scaling of electron density and CT number to materials providing considerably more attenuation then bone.

The scanner was operated in extended-range mode to image an electron density phantom (CIRS Model 062, Norfolk Virgina) including inserts of titanium (6 mm diameter) and stainless steel (8 mm diameter). The clinically-utilised CT-ED curve is obtained at 120 kV and 200 mA, at which titanium and stainless steel would normally saturate the attenuation reconstruction. CT-ED curves were obtained at 120 kV and for a range of tube mA values. Electron density inserts in the CIRS phantom comprised electron densities relative to water (ρ_e^w) ranging from low-density lung (ρ_e^w = 0.2) to titanium (ρ_e^w = 3.7) and stainless steel (ρ_e^w = 6.7). These results are shown in Figure 1. Similar CT-ED curves were also obtained for a variety of kV settings and a tube current of 200 mA, and are shown in Figure 2. It should be noted that with the narrow metal inserts, the artefacts they produced were minimal.

Auto-mA

The auto-mA function utilised by the GE Lightspeed scanner provides mA modulation during scanning at up to 40 Hz based on patient dimensions extracted from scout images[§]. The influence of the auto-mA function on the derived CT-ED relationship was investigated by scanning a phantom with deliberate dimensional changes, designed to produce a large variation in mA. The phantom, shown in Figur 3, is 300 mm wide and was constructed of 40 mm thick solid water slabs (Gammex RMI, Middleton WI). The second slab was made of wax with a hollow section in which various material inserts could be placed. Inserts were manufactured from solid water, polystyrene, aluminium and a bone analogue material composed of cured polyurethane resin with mineral additives** ('Renshape BM 5272', Huntsman Advanced Materials GmbH, Basel)[††]. These inserts had a cross-sectional area of 20 mm × 40 mm and ran the length of the phantom. It was assumed that their material properties are uniform along their length.

The phantom was scanned with the standard tube settings (120 kV, 200 mA) as well as with the auto-mA

[†] *Note, now called "Calvary Mater Newcastle Hospital"*
[‡] *Information from scanner user-manuals and GE website, www.ge.com*
[§] *Information from GE website, www.ge.com*
[**] *The actual composition is subject to proprietary confidentiality*
[††] *Supplied by Bayly (previously P-Type), Blackburn, Victoria*

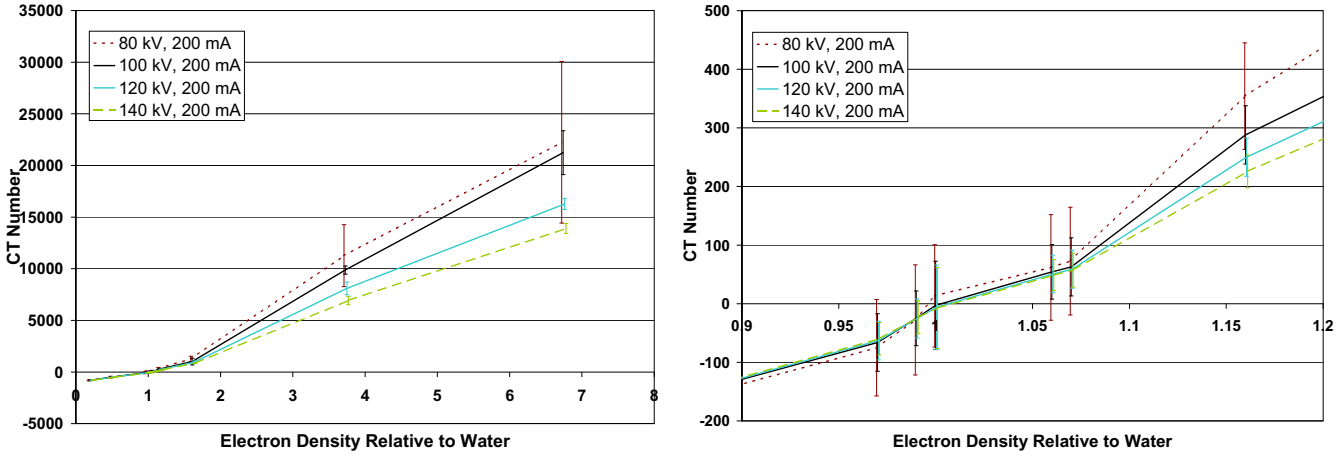

Figure 2. *CT-ED curves derived from images of the CIRS phantom with a variety of inserts, for varying kV settings and a constant tube current of 200 mA. a) Across the full range of relative electron densities considered. b) A magnification of the anatomically-relevant region of the curves.*

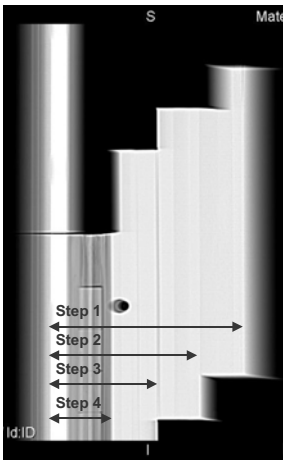

(a) Lateral scout

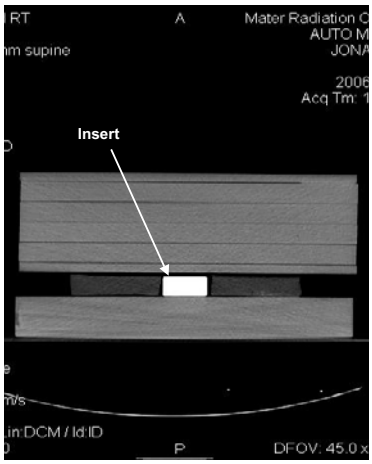

(b) Axial slice

Figure 3. *Phantom constructed for testing the effect of the auto-mA function. Lateral scout and a single axial slice are shown. The scout indicates the 'steps' of the phantom.*

function turned on. The variation in mA at each 'step' of the phantom (see Figure 3) was noted from the resulting DICOM image headers, and this variation with the varying material inserts in place is indicated in Figure 4. Again, CT numbers and variations were obtained by examination of image regions occupied by each material insert, within the region of each 'step' in the phantom, and these results are shown in Figure 5.

Discussion

kV, mA and electron density

Scans undertaken of the phantom with titanium and stainless steel inserts in place, whilst providing images with similar quality for low-density materials, showed considerable noise within the actual metal volume. This is revealed in the standard deviations of CT values recorded in the titanium and stainless steel volumes and shown as error bars in Figure 1 and Figure 2, particularly at low kV. These figures show some divergence from linearity for CT-ED relationship from anatomical densities with increasing relative electron density, consistent with previous observations[4, 13], with material atomic number influencing relative attenuation due to enhanced photoelectric absorption.

Consistency was maintained in CT number for titanium and stainless steel with variation in mA for fixed kV (Figure 1) except for the lowest mA setting. With variation in kV however, a consistent and substantial variation in CT number occurs with CT values reducing with increasing kV, reflecting the diminishing influence of photoelectric absorption. Some variation is also observed for the highest density anatomical material (cortical bone), though it is minor in comparison.

Variations in CT number of over 5000 HU for the titanium and stainless steel samples (as in Figure 2) will have implications for radiotherapy dose calculations,

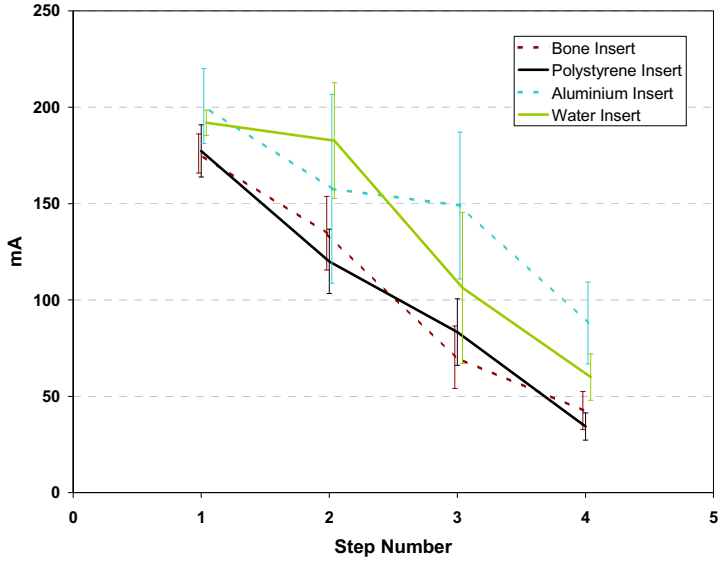

Figure 4. *Variation in automatically selected mA with step for various insert materials.*

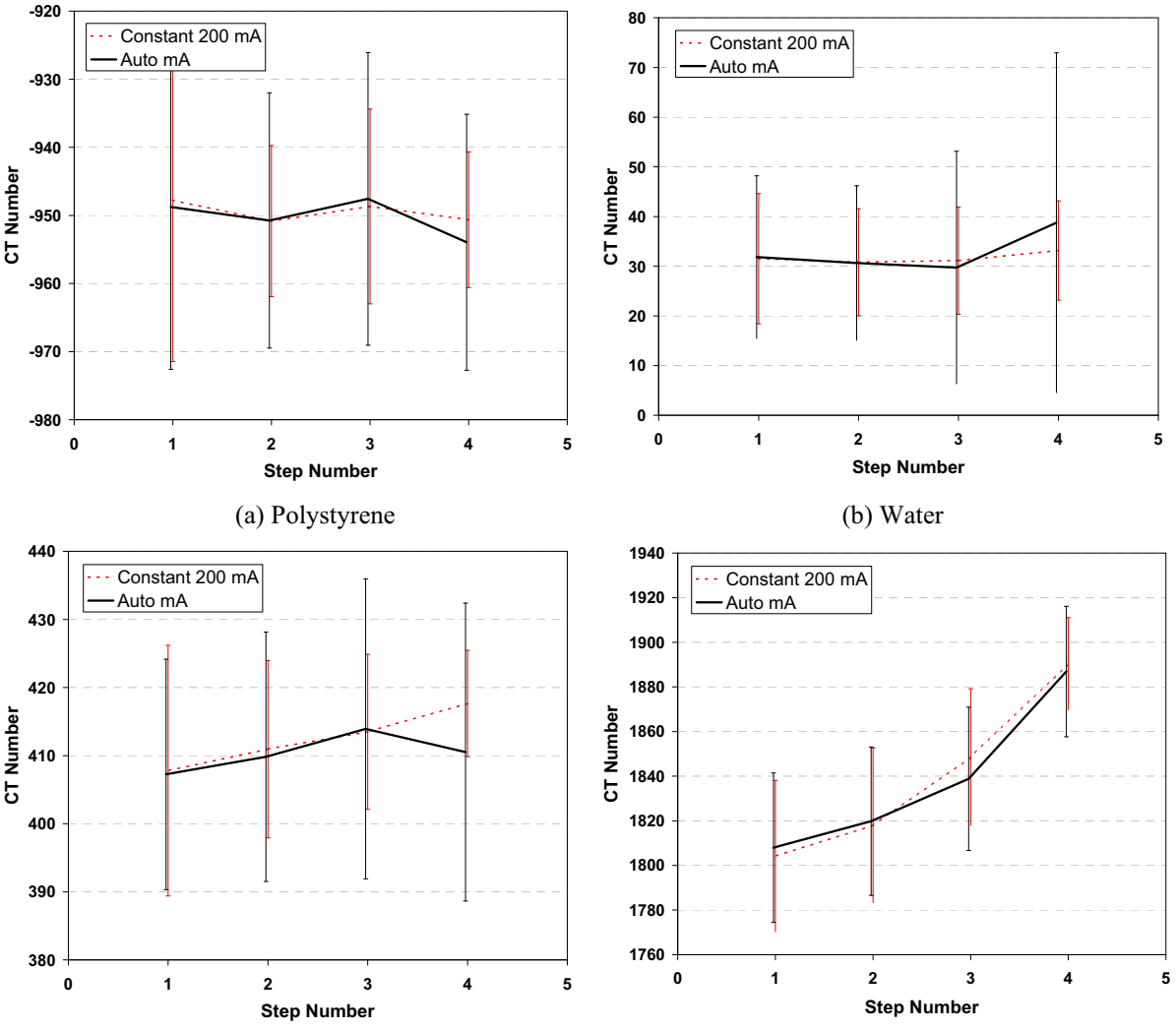

Figure 5. *Variation in CT number with position along the phantom according to the material insert used in each scan with automatic mA adjustment turned on (see Figure 4).*

though this variation is dependent on the planning algorithm used, the positioning and geometry of the implant and other local geometric features[13, 14]. Thomas[1] showed that for soft tissues, ED-CT conversions are virtually independent of CT scanner or scanner settings. For higher density and atomic number anatomic materials (e.g., bone), scanner settings influence the resulting ED-CT relationship, though typically with only minimal affect on subsequent dose calculations. For the high-density materials considered here, the variation in CT number with beam kV will lead to significant variations in dose calculation – of the order of 10 % variation in depth-dose behind a 2 cm insert at 10 cm depth in a 6 MV beam[1].

The dosimetric influence of a large prosthesis – a hip prosthesis for example – is known to be most significant in the tissue regions immediately adjacent to the prosthesis, with variations in attenuation for beams passing through the prosthesis altering resulting dose distributions and monitor unit calculations[5, 15-18]. It has been shown though that for multi-field pelvic treatments, the variation in dose-volume parameters when not correctly accounting for prosthesis attenuation are not substantial[16]. Given the variation shown in Figure 2, and uncertainty in actual dose distribution behind a prosthesis, we recommend that kV settings be considered when scanning high-density materials and consistency maintained between the scan and previously obtained CT-ED curves.

Auto-mA

Automatic tube current modulation provided a substantial variation in mA across the phantom as shown in Figure 4. The variation in mA with position in the phantom changed little with insert type and certainly does not show any consistent relationship to insert material. As shown in Figure 5, CT numbers for insert materials were very similar at all positions along the phantom, for both fixed and modulated mA scanning. The variations in CT number at each position, indicated by error bars for each measurement, shows material definition by CT number is similar for both fixed and modulated mA scanning. These results suggest that auto-mA scanning is suitable for derivation of images for radiotherapy planning applications, without influencing CT-ED relationships. One trend that can be observed is that of an increase in CT number with decreasing phantom thickness, particularly for the aluminium insert (Figure 5d). This trend is the same for fixed and modulated tube current. It can be expected that the results presented here would depend in part on the size and shape of the phantom. This dependency was not examined in detail.

The use of automatic tube current modulation for obtaining images for radiotherapy treatment planning has several advantages[7-12, 17]. The reduction in patient exposure allows reduction in the effective dose to patients. Although this may not be of such relevance for patients about to receive high-dose radiation therapy, ALARA principles require responsible dose reduction. This is also conducive to the acquisition of high-resolution patient images with narrow slice spacing, essential for high-resolution patient localisation and the production of quality digitally-reconstructed radiographs. It is also advantageous for maintaining CT doses when multiple images are obtained, for example when acquiring multiple image sets for multiple phases of the respiratory cycle. Another substantial benefit of automatic tube modulation is that the aim is to generally *reduce* tube mA whilst maintaining image quality. This reduces the current-time of the tube and can lead to extended tube life[10].

Conclusions

This study showed that, although extended range (16-bit) scanning can provide electron density information for materials with densities above the conventional range (obtained with 12-bit imaging), variation in attenuation with X-ray energy leads to variation in CT number with tube kV setting. The resulting variations in CT number should be considered if using default CT-ED tables for treatment planning. The minimal variation in CT number during scanning with automatic tube-current modulation suggests that automatic tube-current modulation is suitable for patient CT scanning for radiotherapy treatment planning purposes.

Acknowledgements

The authors are very grateful to Ms Sue McKay for assistance with preparation of materials for the construction of the phantom.

References

1. Thomas, S.J., *Relative electron density calibration of CT scanners for radiotherapy treatment planning,* The British Journal Of Radiology, 72(860): 781-786, 1999.
2. Metcalfe, P., Kron, T. and Hoban, P., *The Physics of Radiotherapy X-rays from Linear Accelerators*, Medical Physics Publishing, Madison WI, 1997.
3. Schneider, U., Pedroni, E. and Lomax, A., *The calibration of CT Hounsfield units for radiotherapy treatment planning,* Physics In Medicine And Biology, 41(1): 111-124, 1996.
4. Coolens, C. and Childs, P.J., *Calibration of CT Hounsfield units for radiotherapy treatment planning of patients with metallic hip prostheses: the use of the extended CT-scale,* Physics in Medicine & Biology, 48(11): 1591-603, 2003.
5. Keall, P.J., Chock, L.B., Jeraj, R., Siebers, J.V. and Mohan, R., *Image reconstruction and the effect on dose calculation for hip prostheses,* Medical Dosimetry, 28(2): 113-7, 2003.
6. Yazdi, M., Gingras, L. and Beaulieu, L., *An adaptive approach to metal artifact reduction in helical computed tomography for radiation therapy treatment planning: experimental and clinical studies.[erratum appears in Int J Radiat Oncol Biol Phys. 2005 Oct 1;63(2):651 Note: Yazdia, Mehran [corrected to Yazdi, Mehran]],* International Journal of Radiation Oncology, Biology, Physics, 62(4): 1224-31, 2005.
7. Gies, M., Kalender, W.A., Wolf, H. and Suess, C., *Dose reduction in CT by anatomically adapted tube current modulation. I. Simulation studies,* Medical Physics, 26(11): 2235-2247, 1999.
8. Greess, H., Wolf, H., Baum, U., Lell, M., Pirkl, M., Kalender, W.A. and Bautz, W.A., *Dose reduction in computed tomography by attenuation-based on-line modulation of tube*

current: evaluation of six anatomical regions, European Radiology, 10(2): 391-394, 2000.
9. Kalender, W.A., Wolf, H. and Suess, C., *Dose reduction in CT by anatomically adapted tube current modulation. II. Phantom measurements,* Medical Physics, 26: 2248-2253, 1999.
10. Kalra, M.K., Maher, M.M., Toth, T.L., Kamath, R.S., Halpern, E.F. and Saini, S., *Comparison of Z-axis automatic tube current modulation technique with fixed tube current CT scanning of abdomen and pelvis,* Radiology, 232(2): 347-353, 2004.
11. Kalra, M.K., Maher, M.M., Toth, T.L., Kamath, R. S., Halpern, E.F. and Saini, S., *Radiation from "extra" images acquired with abdominal and/or pelvic CT: effect of automatic tube current modulation,* Radiology, 232(2): 409-414, 2004.
12. Kalra, M.K., Maher, M.M., Toth, T.L., Schmidt, B., Westerman, B.L., Morgan, H.T. and Saini, S., *Techniques and applications of automatic tube current modulation for CT,* Radiology, 233(3): 649-657, 2004.
13. Chu, J.C., Ni, B., Kriz, R. and Amod Saxena, V., *Applications of simulator computed tomography number for photon dose calculations during radiotherapy treatment planning,* Radiotherapy & Oncology, 55(1): 65-73, 2000.
14. Purdy, J.A., *Photon dose calculations for three-dimensional radiation therapy,* Seminars in Radiation Oncology, 2: 235-245, 1992.
15. Biggs, P.J. and Russell, M.D., *Effect of a femoral head prosthesis on megavoltage beam radiotherapy,* International Journal of Radiation Oncology, Biology, Physics, 14(3): 581-6, 1988.
16. Keall, P.J., Siebers, J.V., Jeraj, R. and Mohan, R., *Radiotherapy dose calculations in the presence of hip prostheses,* Medical Dosimetry, 28(2): 107-12, 2003.
17. Carolan, M., Dao, P., Fox, C. and Metcalfe, P., *Effect of hip prostheses on radiotherapy dose,* Australasian Radiology, 44(3): 290-5, 2000.
18. Reft, C., Alecu, R., Das, I.J., Gerbi, B.J., Keall, P., Lief, E., Mijnheer, B.J., Papanikolaou, N., Sibata, C. and Van Dyk, J., *Dosimetric considerations for patients with HIP prostheses undergoing pelvic irradiation. Report of the AAPM Radiation Therapy Committee Task Group 63,* Medical Physics, 30(6): 1162-1182, 2003.